Jurnal Sainstech Nusantara	Vol. 2 No. 4 (2025) 51-59
https://nusantarajournal.id/sainstech	ISSN: 3063-0657

Corrosion Rate and Microstructural Evolution of Aluminum 2024-T3 in Nitric Acid under Various Heat Treatment Conditions

Gandhy Priyageng Bhagaskara[1], Ajeng Wulansari[1]

[1]Aircraft Engineering Study Program, Surabaya Aviation Polytechnic, Jl. Jemur Andayani I/73 Wonocolo Surabaya, East Java, 60236, INDONESIA

Article Info

Article history:

Received 05 July, 2025
Revised 19 October, 2025
Accepted 11 November, 2025

Abstract

Aluminum alloy 2024-T3 is widely applied in aerospace structures due to its high strength-to-weight ratio, yet its corrosion behavior in aggressive acidic environments requires further optimization. This study evaluates the influence of heat treatment duration at 300 °C on the corrosion rate and microstructural evolution of Aluminum 2024-T3 immersed in 68% nitric acid (HNO_3). Specimens were prepared under four conditions: without heat treatment and with heat treatment for 1, 2, and 3 hours followed by water quenching. Corrosion testing was conducted using the ASTM G31-72 immersion method at exposure times of 168, 336, 504, and 672 hours, and corrosion rates were determined using the weight loss method, complemented by optical microstructural observation. The results indicate a progressive increase in corrosion rate with immersion time for all specimens. Untreated samples exhibited the highest corrosion rate, reaching 480.88 mpy at 672 hours, whereas heat-treated specimens demonstrated reduced corrosion rates, with the lowest value of 365.03 mpy observed in the 1-hour treatment condition, corresponding to an overall reduction of up to 11.70%. Microstructural analysis revealed a transition from dominant pitting corrosion in untreated specimens to intergranular corrosion in heat-treated samples. These findings highlight the role of thermal processing in enhancing corrosion resistance and optimizing service performance in acidic environments.

Keyword: Aluminum 2024-T3, Heat treatment, Nitric acid (HNO_3), Corrosion rate; Immersion testing, Microstructural analysis

Corresponding Author:

Ajeng Wulansari
Email: ajeng.wulansari@poltekbangsby.ac.id

1. Introduction

Aluminum alloy 2024-T3 is among the most widely deployed high-strength aluminum alloys in aerospace structures due to its excellent strength-to-weight ratio, good fatigue resistance, and reliable formability. As an Al–Cu–Mg alloy, AA2024 derives its mechanical performance from

DOI: https://doi.org/10.71225/jstn.v2i4.122

precipitation hardening, while the T3 temper achieved through solution treatment, quenching, and natural aging—enhances strength without excessive loss of ductility. Despite these advantages, corrosion remains a persistent engineering problem in aircraft service, where chemical exposure and surface degradation can compromise structural integrity, elevate maintenance cost, and shorten component lifetime.

Corrosion of AA2024 is strongly governed by microstructural heterogeneity, particularly the distribution of Cu-rich intermetallics and grain boundary features that may act as preferential dissolution sites. In aggressive acidic environments, aluminum alloys can undergo localized attack such as pitting corrosion and intergranular corrosion, and the dominant mechanism may shift depending on exposure duration and metallurgical condition. Because thermal history influences precipitation, grain boundary chemistry, and residual stress, heat treatment is frequently considered as an engineering route to tune corrosion resistance while maintaining mechanical properties.

State of the art indicates that corrosion studies on AA2024 have been conducted across several corrosive media and methodological approaches. Immersion-based evaluation using the ASTM G31-72 weight loss method remains a common benchmark for quantifying corrosion rate over time, often complemented by surface/microstructure observations. Prior work has shown that immersion duration generally accelerates mass loss and corrosion rate progression, and that procedural factors (e.g., rinsing/cleaning during exposure) can substantially reduce apparent corrosion rate. Other studies have examined the influence of heat treatment under acidic conditions particularly hydrochloric acid reporting that thermally treated specimens may exhibit lower corrosion rates than untreated ones, although the magnitude varies with temperature, duration, and quenching practice. Additionally, comparative investigations across media (HCl, HNO_3, and NaCl) suggest that nitric acid can induce notable corrosion severity and distinct corrosion morphologies, yet most available reports focus on shorter immersion windows or do not systematically isolate heat-treatment time as a key variable in highly concentrated nitric acid.

Despite this growing body of research, two gaps remain evident. First, studies that specifically combine concentrated nitric acid (68% HNO_3) with controlled heat treatment duration at a fixed temperature are still limited, particularly for prolonged exposure up to 672 hours using standardized immersion practice. Second, the mechanistic linkage between heat-treatment time, corrosion rate evolution (mpy), and the resulting shift in corrosion mode (e.g., from pitting to intergranular features) has not been adequately clarified under nitric-acid-dominated conditions.

Therefore, this study investigates the effect of heat treatment duration at 300 °C (1, 2, and 3 hours) followed by water quenching on the corrosion behavior of Aluminum 2024-T3 immersed in 68% nitric acid for 168–672 hours. Corrosion performance is quantified via ASTM G31-72 weight loss measurements and supported by optical microstructural observation. The findings are expected to strengthen understanding of how thermal processing modulates corrosion kinetics and corrosion morphology, offering practical insights for optimizing heat-treatment parameters to improve service durability of aerospace-grade aluminum in aggressive acidic environments.

2. Research Method

2.1 Material Preparation

The material used in this study was Aluminum Alloy 2024-T3 in sheet form. The specimens were machined into rectangular plates with dimensions of 17 mm × 10 mm × 2 mm. A total of 16 specimens were prepared and divided into four experimental groups: (1) without heat treatment (control), and (2–4) with heat treatment durations of 1, 2, and 3 hours at 300 °C. Prior to testing, all specimens were mechanically cleaned, rinsed with distilled water, and dried to remove surface

DOI: https://doi.org/10.71225/jstn.v2i4.122

contaminants. The initial mass of each specimen was measured using a digital analytical balance with high precision and recorded for corrosion rate calculation.

Heat treatment was performed in an electric furnace at a constant temperature of 300 °C. Specimens assigned to the heat-treated groups were heated for 1, 2, and 3 hours, respectively. After reaching the designated holding time, specimens were removed from the furnace and immediately quenched in distilled water for 5 minutes to stabilize the microstructure. The untreated group was not subjected to any thermal modification and served as the reference condition. This controlled thermal variation allowed evaluation of the influence of heat treatment duration on corrosion behavior.

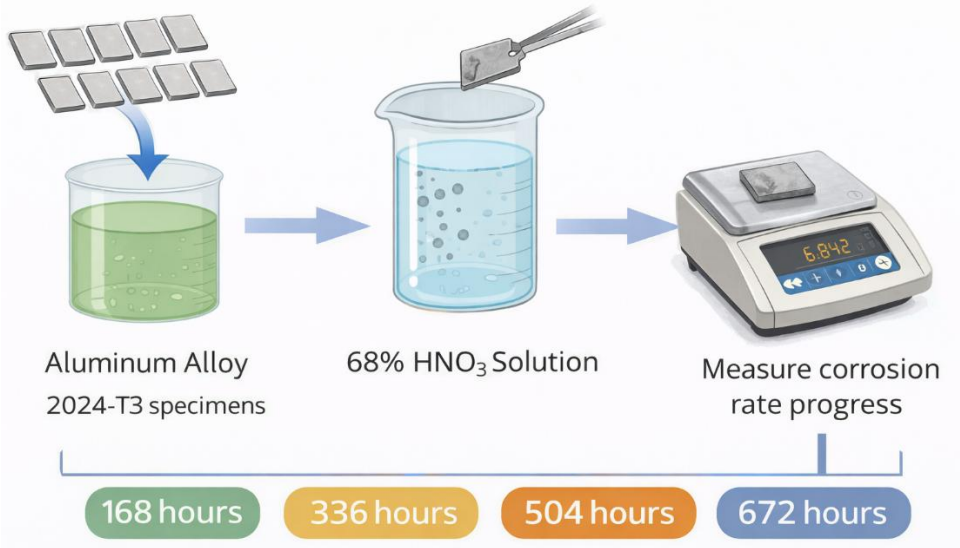

Figure 1. Material Preparation

2.2 Corrosion Testing

Corrosion testing was conducted using the immersion method in accordance with ASTM G31-72 standard practice. A nitric acid (HNO_3) solution with a concentration of 68% was used as the corrosive medium. Each specimen was immersed individually in 90 mL of nitric acid solution contained in glass vessels to prevent cross-contamination. Immersion durations were set at 168, 336, 504, and 672 hours to evaluate corrosion rate progression over time. During immersion, containers were sealed to minimize contamination and evaporation. After each designated exposure period, specimens were removed, rinsed with distilled water to eliminate residual acid, dried, and reweighed to determine mass loss. Corrosion rate was determined using the weight loss method based on ASTM G31-72. The corrosion rate (CR) in mils per year (mpy) was calculated using:

$$CR = \frac{(K \times W)}{A \times T \times D}$$

where:
CR = corrosion rate (mpy)
K = constant (3.45×10^6 for mpy)
W = weight loss (g)
A = exposed surface area (cm^2)
T = exposure time (hours)
D = material density (g/cm^3)

DOI: https://doi.org/10.71225/jstn.v2i4.122

2.5 Microstructural Observation

Microstructural characterization was carried out using a reflected-light optical microscope equipped with a Dino Eye digital camera system (CMOS sensor, high-resolution imaging up to 5 MP) connected to a computer for real-time visualization and image acquisition. Observations were performed under bright-field reflected illumination with adjustable LED light intensity to enhance surface contrast and morphological clarity. Magnifications of 50×, 100×, 200×, and 400× were employed to examine both general surface degradation and localized corrosion features. Prior to microscopic examination, specimen surfaces were prepared following standard metallographic procedures. After immersion testing, specimens were rinsed with distilled water to remove residual nitric acid, followed by ultrasonic cleaning in distilled water for 5 minutes to eliminate loose corrosion products. Samples were then air-dried at room temperature. For clearer microstructural visualization, selected specimens were ground sequentially using silicon carbide (SiC) abrasive papers (grit 400, 600, 800, and 1200), followed by polishing with alumina suspension (1 μm particle size) to obtain a mirror-like surface finish. No chemical etching was applied in order to preserve corrosion morphology.

3. Results And Discussion

3.1 Effect of Heat Treatment Duration on Weight Loss Behavior

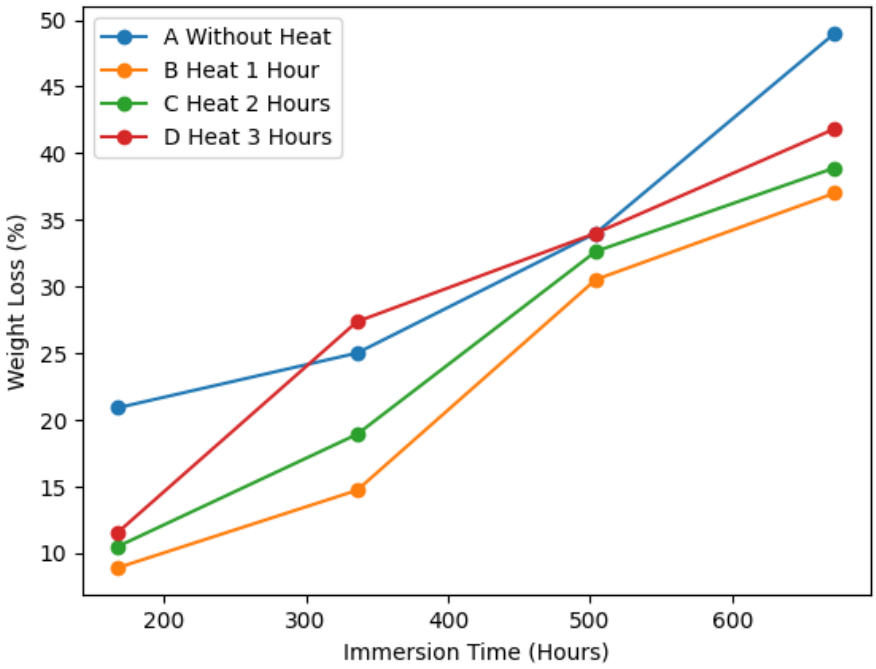

Figure 2. Weight Loss vs Immersion time

Figure 2 shows a clear time-dependent increase in weight loss percentage for all Aluminum 2024-T3 specimens immersed in 68% HNO_3 for 168–672 hours, indicating that immersion duration is the dominant factor controlling material degradation. The untreated specimen exhibited the highest weight loss at all exposure intervals, rising from 20.9% at 168 hours to 49% at 672 hours, accompanied by a corrosion rate reaching 480.88 mpy. The most pronounced acceleration occurred between 504 and 672 hours, suggesting intensified dissolution during prolonged exposure. In contrast, heat-treated specimens consistently showed lower degradation levels, with the 1-hour

DOI: https://doi.org/10.71225/jstn.v2i4.122

treatment condition demonstrating the best performance (37% weight loss and 365.03 mpy at 672 hours), corresponding to an overall reduction of approximately 11.70% compared to the control. Specimens treated for 2 and 3 hours exhibited slightly higher corrosion rates (369.37 and 395.45 mpy, respectively), indicating that excessive holding time may partially reduce the protective effect of thermal modification.

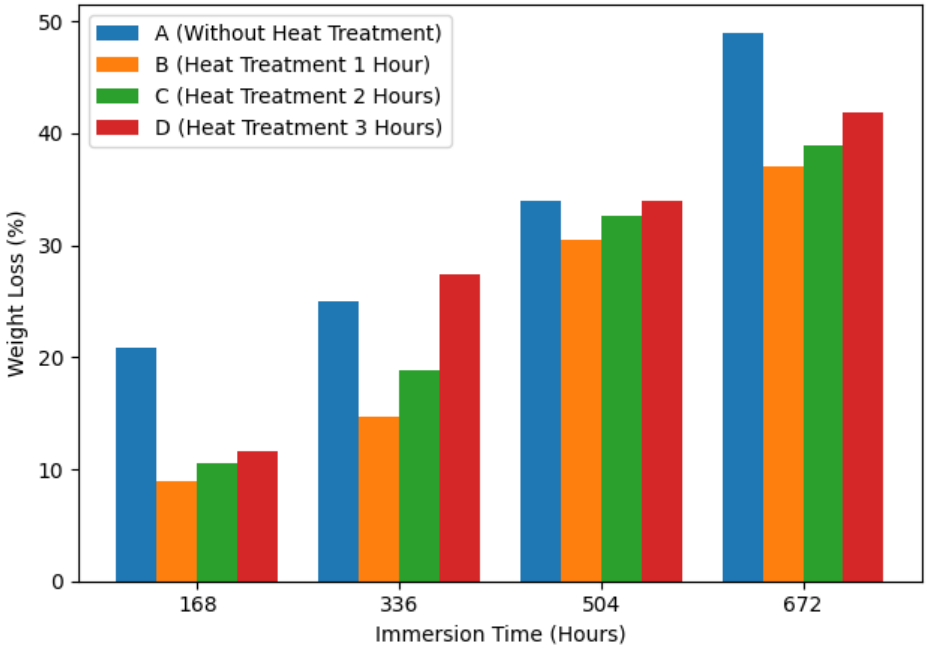

Figure 3. (a) Percentage Weight Loss Sample (b) Comparasion Weight Loss

From a kinetic perspective, the continuous increase in corrosion rate with time suggests a non-linear behavior consistent with a power-law relationship ($CR \propto t^n$), where corrosion accelerates rather than stabilizes, implying the absence of long-term passivation. In concentrated nitric acid, the native Al_2O_3 passive film undergoes repeated breakdown and repassivation cycles; however, aggressive oxidizing conditions promote sustained anodic dissolution, preventing the establishment of a stable protective layer. Microstructural observations revealed dominant pitting corrosion in untreated specimens, characterized by localized cavity formation that intensified over time. Heat-treated samples, however, showed a transition toward intergranular corrosion, indicating that thermal exposure modified grain boundary chemistry and electrochemical heterogeneity. This behavior is closely linked to the redistribution and precipitation of Cu-rich θ-phase (Al_2Cu) particles during heating at 300 °C. Short-duration heat treatment likely promotes more homogeneous precipitate dispersion and partial stress relief, reducing galvanic coupling intensity between the aluminum matrix (anodic) and intermetallic particles (cathodic). Conversely, prolonged treatment may induce precipitate coarsening or grain boundary segregation, increasing susceptibility to intergranular attack despite overall lower corrosion rates than the untreated condition.

Collectively, these results demonstrate that corrosion performance of AA2024-T3 in concentrated nitric acid is governed by the interplay between time-dependent electrochemical dissolution, passive film instability, and heat-treatment-induced microstructural evolution. Controlled thermal processing, particularly at 300 °C for 1 hour, provides an optimal balance between microstructural stability and corrosion resistance, highlighting the critical role of metallurgical conditioning in enhancing durability of high-strength aluminum alloys in aggressive acidic environments relevant to aerospace applications.

DOI: https://doi.org/10.71225/jstn.v2i4.122

3.2 Microstructural Analysis

Microstructural observations were conducted using a Dino Eye optical microscope to evaluate surface degradation of Aluminum 2024-T3 specimens after immersion in nitric acid (HNO_3). The micrographs presented in Figure 4 and figure 5. reveal substantial differences in corrosion morphology as a function of heat treatment duration and immersion time. These qualitative observations are fully consistent with the quantitative weight loss and corrosion rate data, confirming that microstructural evolution governs the degradation mechanism in acidic environments.

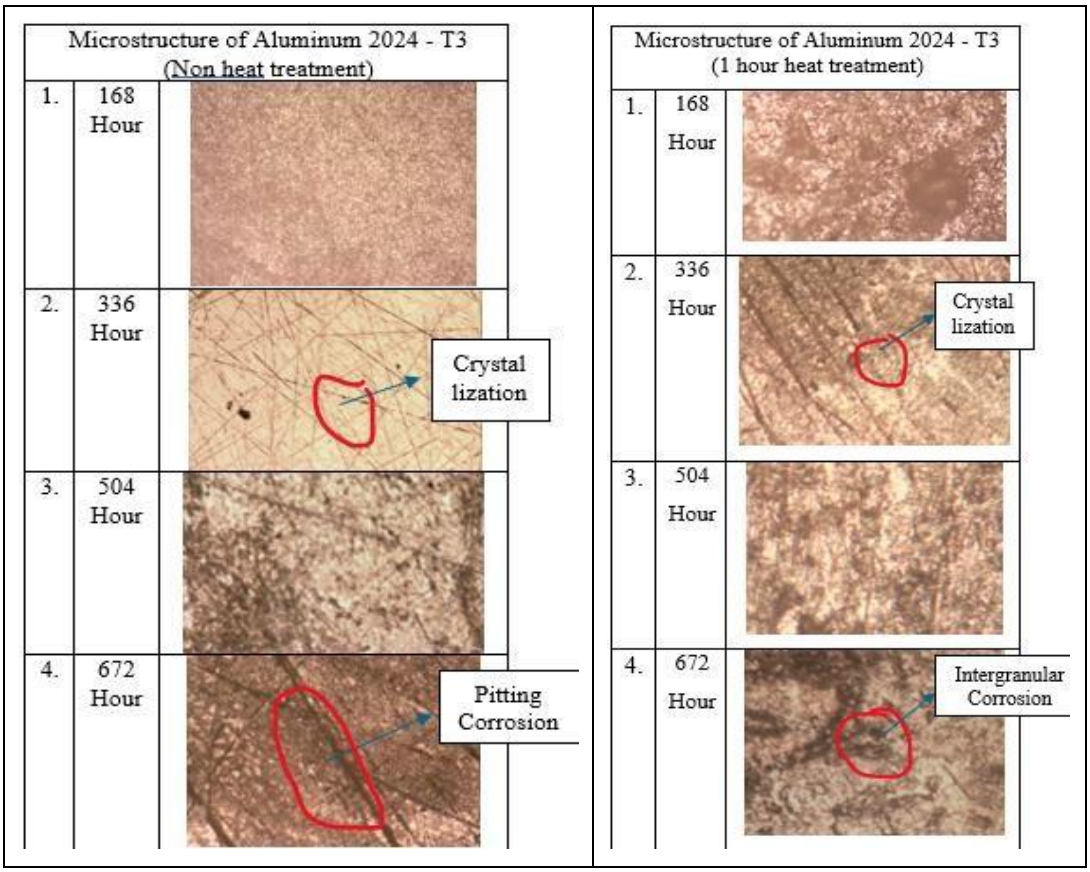

Figure 4. Microstructural Analysis (a) untreatment (b) 1 hour treatment

For the non-heat-treated specimens, the surface at 168 h remained relatively intact, with no pronounced corrosion features. However, after 336 h of immersion, surface crystallization became visible, indicating the formation of corrosion products and the onset of localized electrochemical activity. At 672 h, the surface was dominated by pronounced pitting corrosion. The pits appeared deep and localized, reflecting breakdown of the naturally formed passive oxide layer in the aggressive HNO_3 environment. From a metallurgical standpoint, Aluminum 2024-T3 contains a significant Cu fraction (3.8–4.9 wt%), leading to the presence of Al_2Cu intermetallic particles. These particles act as cathodic sites relative to the aluminum matrix, establishing micro-galvanic cells. The potential difference between the Cu-rich precipitates and the surrounding matrix accelerates localized anodic dissolution, thereby promoting pitting corrosion. This explains the sharp increase in corrosion rate and weight loss observed in the non-heat-treated specimens at extended immersion times. In contrast, specimens subjected to heat treatment at 300 °C for 1, 2, and 3 hours followed by water quenching exhibited a distinct corrosion morphology. At 168 h, the surfaces remained comparatively stable, suggesting improved microstructural homogeneity and reduced residual stresses due to thermal exposure. At 336 h, corrosion features appeared more uniformly distributed,

DOI: https://doi.org/10.71225/jstn.v2i4.122

indicating a transition toward generalized surface attack. After 672 h of immersion, intergranular corrosion became the dominant mechanism. Corrosion propagation along grain boundaries suggests that heat treatment altered precipitate distribution, particularly through redistribution and coarsening of Al_2Cu phases. The formation of precipitate-free zones (PFZs) adjacent to grain boundaries creates localized compositional gradients, rendering these regions anodically susceptible. Consequently, corrosion preferentially follows grain boundary networks rather than forming isolated pits.

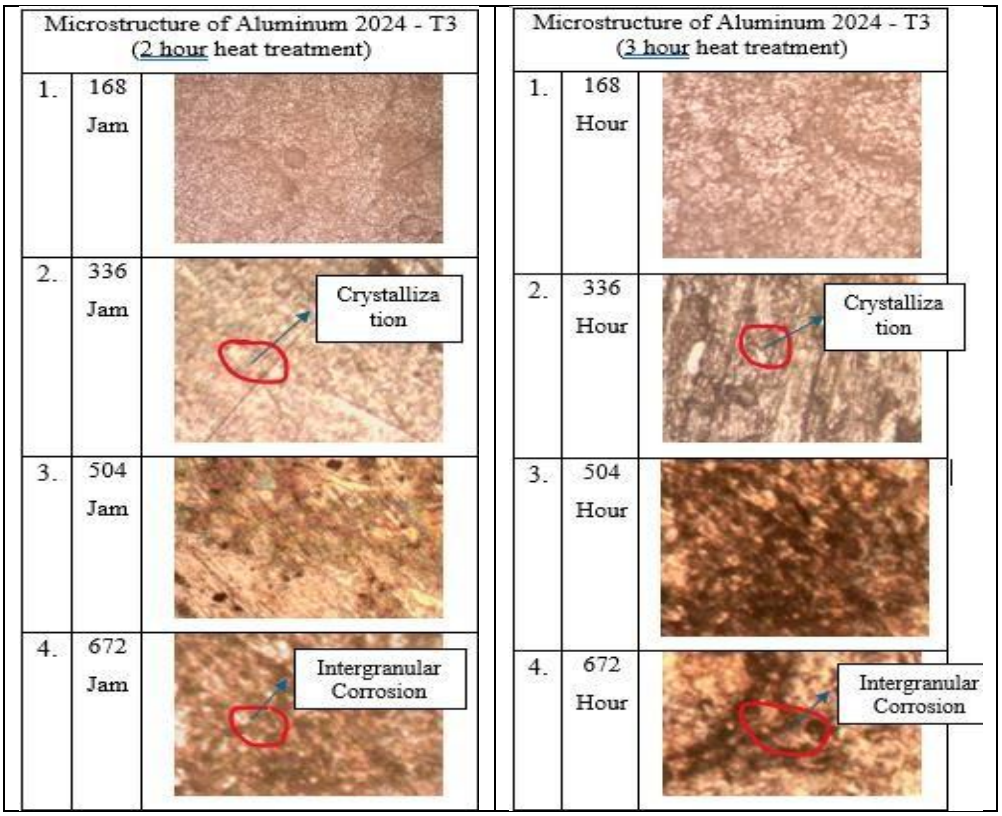

Figure 5. Microstructural Analysis (a) 2 hour treatment (b) 3 hour treatment

The transition from pitting corrosion in the untreated condition to intergranular corrosion in heat-treated specimens is mechanistically significant. Although intergranular corrosion remains detrimental, it generally progresses in a more distributed manner compared to highly penetrative pitting attack. This difference in corrosion mode explains the lower corrosion rates measured in heat-treated specimens, particularly at 672 h. Heat treatment reduces extreme micro-galvanic coupling by promoting a more uniform phase distribution, thereby mitigating severe localized dissolution. An important finding of this study is that heat treatment at 300 °C does not eliminate corrosion but fundamentally modifies its mechanism and kinetics. While prolonged immersion inevitably increases corrosion severity, thermal treatment effectively reduces the overall corrosion rate and alters the dominant degradation pathway from aggressive pitting to comparatively controlled intergranular attack. This mechanistic shift is critical for aerospace applications, where localized pitting can act as stress concentrators and initiate crack propagation under cyclic loading. The results therefore demonstrate that controlled thermal processing can enhance corrosion performance of Aluminum 2024-T3 in nitric acid environments by stabilizing its microstructure and moderating electrochemical heterogeneity. Overall, the combined microstructural and gravimetric evidence establishes a direct correlation between heat treatment, precipitate evolution, and corrosion morphology. The findings

DOI: https://doi.org/10.71225/jstn.v2i4.122

highlight that microstructural engineering is a decisive parameter in controlling corrosion behavior of high-strength Al–Cu alloys exposed to aggressive acidic media.

4. Conclusion

This study examined the corrosion performance and microstructural evolution of Aluminum 2024-T3 exposed to highly concentrated nitric acid (68% HNO_3) under different heat-treatment durations at 300 °C followed by water quenching, using ASTM G31-72 immersion testing over 168–672 h. Across all conditions, corrosion severity increased monotonically with immersion time, confirming that prolonged exposure in strongly oxidizing acid prevents the formation of a stable, long-term protective film and sustains anodic dissolution. The untreated condition consistently exhibited the greatest degradation, reaching 480.88 mpy at 672 h with a maximum mass-loss level of 49%. In contrast, heat-treated specimens showed reduced corrosion rates at all immersion intervals, demonstrating that controlled thermal processing can mitigate corrosion kinetics in HNO_3. The most effective parameter set in this work was 300 °C for 1 h, which produced the lowest corrosion rate at 672 h (365.03 mpy) and a reduced mass loss (37%), corresponding to an overall reduction of up to 11.70% relative to the untreated specimen. Heat treatments of 2 h and 3 h also improved performance compared to the control, but exhibited slightly higher corrosion rates than the 1-h condition at long exposure, suggesting that excessive holding time may promote precipitate coarsening and grain-boundary susceptibility. Microstructural observations provide a mechanistic explanation for these kinetic trends. The untreated specimen evolved toward dominant pitting corrosion, whereas heat-treated specimens exhibited a shift toward intergranular corrosion at extended immersion (672 h). This transition indicates that heat treatment altered micro-galvanic heterogeneity and redistributed Cu-rich phases (e.g., Al_2Cu), reducing severe localized pit development but increasing grain-boundary-related attack pathways. Importantly, the study's key contribution is not merely the reduction in corrosion rate, but the clear evidence that heat treatment changes the dominant corrosion mode a finding that is practically significant for aerospace applications, where deep pitting can act as critical crack-initiation sites under cyclic loading.

Acknowledgements

The authors gratefully acknowledge the Surabaya Aviation Polytechnic and the Aircraft Engineering Study Program for providing laboratory facilities and institutional support required to conduct specimen preparation, heat-treatment processing, and immersion corrosion testing. The authors also thank the laboratory technicians and staff for assistance with furnace operation, quenching procedures, mass measurement, and microscopic documentation using the Dino Eye imaging system. Their technical contributions were essential to ensuring experimental consistency and data reliability

References

[1] J. Cao, Y. Wang, G. Xu, X. Liu, X. Zeng, and K. Wei, "Effect of post-weld induction heat treatment on single-pass high-power laser-arc hybrid welded thick stainless steel clad plate: microstructure, mechanical properties and corrosion resistance," *Journal of Materials Research and Technology*, vol. 38, pp. 2623–2635, Sep. 2025, doi: 10.1016/j.jmrt.2025.08.068.

[2] G. Chen *et al.*, "The influence of post-weld heat treatment on the corrosion resistance of CLAM steel weld bead in flowing LBE at 550°C," *Nuclear Engineering and Design*, vol. 444, p. 114418, Dec. 2025, doi: 10.1016/j.nucengdes.2025.114418.

[3] G. Chen *et al.*, "The effects of cold rolling and heat treatment on enhancing molten nitrate corrosion resistance of High-Al 310S stainless steel," *Journal of Materials Research and*

DOI: https://doi.org/10.71225/jstn.v2i4.122

Technology, vol. 39, pp. 2816–2831, Nov. 2025, doi: 10.1016/j.jmrt.2025.10.011.
[4] W. Chen *et al.*, “Corrosion resistance, mechanical and magnetic properties of cold-sprayed Al coating on the sintered NdFeB magnet after heat treatment,” *Journal of Magnetism and Magnetic Materials*, vol. 629, p. 173265, Oct. 2025, doi: 10.1016/j.jmmm.2025.173265.
[5] X. Dang *et al.*, “Corrosion resistance of Ti-1Al-8V-5Fe fabricated via laser powder bed fusion: Effect of post-heat treatment,” *Electrochimica Acta*, vol. 557, p. 148337, May 2026, doi: 10.1016/j.electacta.2026.148337.
[6] S. Gao, B. Zhou, Y. Liu, D. Teng, Y. Xie, and X. Zhang, “Effect of heat treatment on mechanical properties, wear and corrosion resistance of HVAF sprayed FeCoNiCrMo high-entropy alloy coating,” *Materials Characterization*, vol. 226, p. 115199, Aug. 2025, doi: 10.1016/j.matchar.2025.115199.
[7] T. Guo *et al.*, “Corrosion resistance and microstructure of 3D printed magnesium alloy regulated by heat treatment,” *Corrosion Communications*, Oct. 2025, doi: 10.1016/j.corcom.2025.01.004.
[8] Y. Hu *et al.*, “Enhanced corrosion resistance and cellular response of nanostructured Cu-containing TiO_2 coatings via alkali-heat treatment and hydrothermal sterilization,” *Materials Today Communications*, vol. 49, p. 113930, Dec. 2025, doi: 10.1016/j.mtcomm.2025.113930.
[9] M. F. Khan and Z. M. Gasem, “Effect of heat treatment on the passivity and corrosion resistance of steel rebar in simulated cement pore solutions,” *Construction and Building Materials*, vol. 491, p. 142580, Sep. 2025, doi: 10.1016/j.conbuildmat.2025.142580.
[10] Y. Leng *et al.*, “Enhancing corrosion resistance of heat-assisted forming titanium bipolar plate for proton exchange membrane fuel cell through optimized heat treatment,” *Chinese Journal of Chemical Engineering*, vol. 91, pp. 49–59, Mar. 2026, doi: 10.1016/j.cjche.2025.11.007.
[11] M. Li, Y. Zhang, B. Liu, J. Shi, K. Yu, and J. Li, “Mechanism of heat treatment regulation on the formation of Ti-6Al-4V oxide film in additive manufacturing and its corrosion resistance: Synergistic effect of matrix structure and residual stress,” *Corrosion Science*, vol. 263, p. 113721, May 2026, doi: 10.1016/j.corsci.2026.113721.
[12] Z. Li, J. Gou, J. Gao, J. Zhu, W. Kou, and J. Wang, “Microstructural evolution and corrosion resistance of additively manufactured Ti–6Al–4V alloy annular shaped components using multistage heat treatment,” *Materials Chemistry and Physics*, vol. 346, p. 131414, Dec. 2025, doi: 10.1016/j.matchemphys.2025.131414.
[13] M. Sheheryar, D.-M. Chun, and A. G. Abd-Elrahim, “Tailoring corrosion resistance and wettability of AZ31 Mg alloy via laser, hot water, and silicone oil heat treatments,” *Journal of Materials Research and Technology*, vol. 40, pp. 2182–2193, Jan. 2026, doi: 10.1016/j.jmrt.2025.12.248.
[14] M. Song, R. Dong, and T. Xu, “Study on the electrochemical corrosion resistance of 5083 aluminum alloy under heat treatment processes,” *Electrochemistry Communications*, vol. 182, p. 108079, Jan. 2026, doi: 10.1016/j.elecom.2025.108079.
[15] J. Wu *et al.*, “Sc microalloying improved heat and corrosion resistance of an Al-Cu-Mg alloy under varied heat treatment processes,” *Materials Characterization*, vol. 228, p. 115392, Oct. 2025, doi: 10.1016/j.matchar.2025.115392.
[16] C. Zhang *et al.*, “Induced growth orientation deviation of $Mg(OH)_2$ by heat treatment to enhance corrosion resistance of Mg-Sc alloy,” *Corrosion Science*, vol. 257, p. 113271, Dec. 2025, doi: 10.1016/j.corsci.2025.113271.
[17] Q. Zheng *et al.*, “Effect of heat treatment on the microstructure and corrosion resistance of laser powder bed fusion ODS-316L,” *Journal of Materials Research and Technology*, vol. 39, pp. 2134–2142, Nov. 2025, doi: 10.1016/j.jmrt.2025.09.256.
[18] Q. Zhong *et al.*, “In-situ construction of the hydrophobic structure to improve the corrosion resistance on TA1 pure titanium by vacuum heat treatment,” *Surface and Coatings Technology*, vol. 512, p. 132440, Sep. 2025, doi: 10.1016/j.surfcoat.2025.132440.

DOI: https://doi.org/10.71225/jstn.v2i4.122